Journal of the Korean Physical Society, Vol. 74, No. 12, June 2019, pp. 1190∼1196

Study of a New Imaging Strategy Based on Compressed Sensing to Shorten the Imaging Time of a Fourier Telescope

Lei Dong
Changchun Institute of Optics, Fine Mechanics and Physics, Chinese Academy of Sciences, Changchun 130033, China and University of Chinese Academy of Sciences, Beijing 100049, China

Zhenwu Lu, Xinyue Liu, Zhengwei Li and Liang Wang*
Changchun Institute of Optics, Fine Mechanics and Physics, Chinese Academy of Sciences, Changchun 130033, China

(Received 16 January 2019, in final form 19 February 2019)

A Fourier telescope (FT) is an imaging system based on laser illumination and optical aperture synthesis and is suitable for imaging distant targets with high resolution through the atmosphere. The imaging time of a conventional FT is so long (about two hours) as to limit its practical applications. In order to shorten the imaging time of a Fourier telescope, we propose a new imaging system called the compressed sensing Fourier telescope (CS-FT). The image quality, the imaging time and the effects of noise of the new system are studied in detail. Based on the analysis, we find that by reasonably choosing the total sampling rate (TSR), the imaging time of the CS-FT is obviously shorter than that of the conventional FT while the image quality of the CS-FT is near that of the conventional FT. Worth noting is that with the smaller values of the low-frequency sampling rate (LSR) and the order of the sampling probability density function (OPDF), the CS-FT can achieve a better image quality. The reconstruction results of the field data show that the CS-FT can reduce the imaging time of a FT in an actual noise environment.

PACS numbers: 95.55.Cs, 95.75.Rs, 42.30.Kq, 42.30.Va, 42.30.Wb
Keywords: Image detection systems, Fourier telescope, Image reconstruction techniques, Compressed sensing
DOI: 10.3938/jkps.74.1190

I. INTRODUCTION

The Fourier telescope (FT) is an encouraging candidate for imaging small, distant, and dim targets with high resolution, especially for obtaining images of satellites. It is an imaging system based on laser illumination and optical aperture synthesis [1–7] and is not sensitive to the atmospheric turbulence [8, 9]. Potential applications include monitoring geostationary and geosynchronous orbit targets such as done by the GLINT (GEO Light Imaging National Testbed) program [10–12] and imaging the fast-moving low-orbit targets such as done by the SAINT (Satellite Active Imaging National Testbed) program [13–15]. Generally, the diameter of a transmitting laser beam is small, for example, below 40 cm in the GLINT program; therefore, adaptive optics (AO) systems are not needed for correcting the wavefront of the beam with respect to the FT. As a result, the imaging system is simplified and the cost is reduced.

In the process of measurement, the position of the Fourier telescope system relative to the target must remain relatively stationary, so the compression of the imaging time is very important. Although a scheme of simultaneous transmission of three beams may make the system structure simpler, a long time (about two hours) is required because only one Fourier component is measured once.

The recently developed compressed sensing theory [16–20] shows that a sparse or compressible signal can be reconstructed accurately by randomly sparse sampling, which can be used to shorten the imaging time of the FT. Artificial objects usually have a regular structure, which means that they are compressible. Hence, the objects can be accurately reconstructed by using sparse sampling in the Fourier domain, which considerably reduces the number of measurement samples and then reduces the imaging time. Based on the above characteristics, our team combined the conventional Fourier telescope and compressed sensing theory to introduce a new imaging system called the compressed sensing Fourier telescope (CS-FT). As far as we know, research on the CS-FT has rarely been published. Although the

*E-mail: wangliang.ciomp@foxmail.com; Fax: +86-431-84627071

 ©2019 The Korean Physical Society

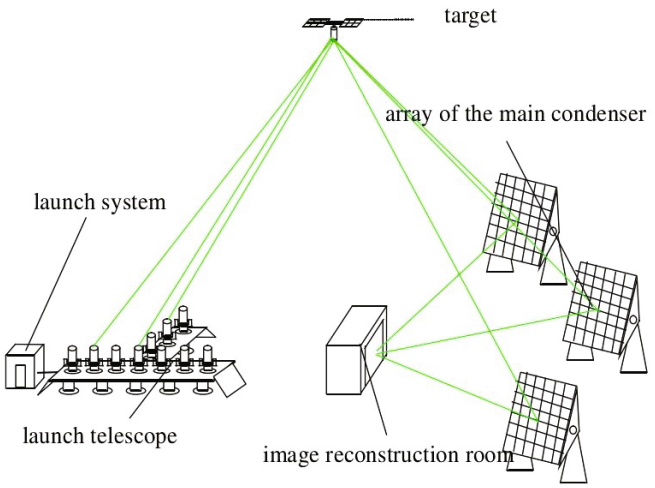

Fig. 1. (Color online) Scheme of the Fourier telescope.

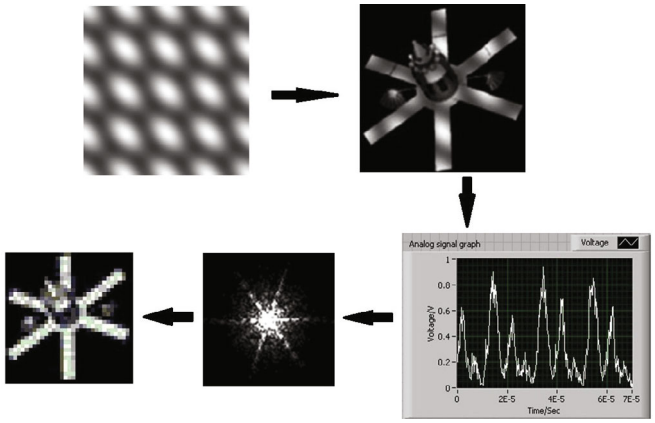

Fig. 2. Scheme of image reconstruction.

CS-FT is somewhat similar to the compressive-sensing-based single-pixel imaging system (CS-SPI) in terms of reducing the amount of sensing data, the mechanisms of sensing data for these two imaging systems vary considerably. Specifically, the CS-FT compresses the data in the spatial-frequency domain while the CS-SPI compresses the data in the spatial domain. Furthermore, the CS-FT also has some particular techniques such as the frequency modulation and the demodulation in the time domain, which are inherited from the conventional FT. In this research, we validated the imaging performance of the CS-FT by using the noisy data of a field experiment, which means that the CS-FT is probably feasible for use as a practical imaging system to some extent. Then, by changing the three main parameters, *i.e.*, the total sampling rate (TSR), the low-frequency sampling rate (LSR) and the order of the sampling probability density function (OPDF), we compare the imaging quality and the imaging time of the CS-FT with those of the conventional FT.

This paper is structured as follows: The second section briefly introduces the imaging principle of the conventional FT. The third section introduces the imaging principle of the CS-FT. The fourth section includes the analysis and the comparison of the imaging quality of both methods. Then, the fifth section includes the simple analysis and comparison of the imaging time of both methods. Finally, the last section concludes the paper.

II. BRIEF INTRODUCTION TO THE FOURIER TELESCOPE

The basic principle of Fourier telescope has been discussed in the literature [21–24] in detail. Its systematic composition and image reconstruction process are shown in Fig. 1 and Fig. 2, respectively. The Fourier telescope transmits three (or more) laser beams to the target at the same time. Different spatial frequency components are produced by changing the baseline configurations. The optical energy receiver collects the light reflected from the target. After the frequency demodulation and the phase closure, the Fourier component corresponding to the transmitting baseline can be obtained. After obtaining enough Fourier components, we can reconstruct the target's image by using an inverse Fourier transform. The main advantages of the Fourier telescope are as follows: (I) the active aperture synthesis, by which tens of meters of effective aperture will be synthesized; (II) the characteristic of immunity to atmospheric turbulence, because of which a complex and expensive adaptive optics system is not needed; (III) the characteristic of encoding spatial information of objects into time domain, because of which a receiving mirror with high optical quality are not needed, with just a large-area energy-receiving mirror (low optical quality) can realize high-resolution imaging.

III. FOURIER TELESCOPE BASED ON COMPRESSED SENSING

As soon as the CS theory was proposed, it was widely used in many applications. One of the most important examples is that the CS method has solved the problem of the long time reconstruction of nuclear magnetic resonance imaging (MRI) [18]. The basic principle of MRI is that the MRI collects the K-spatial data (spatial frequency domain) through special equipment and then reconstructs the image by using an inverse fast Fourier transform (IFFT). This principle is very similar to that of the Fourier telescope. The Fourier telescope obtains all of the spatial spectral components by changing the baseline configuration and then reconstructs the image by using the IFFT. Therefore, we can introduce compressed sensing to the conventional FT and then produce a new imaging system known as the CS-FT.

The CS-FT has several characteristics. Firstly, the

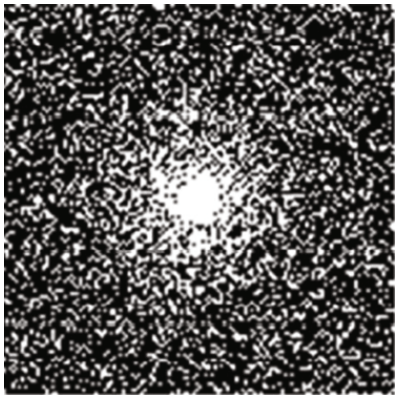

Fig. 3. Randomly sparse sampled template.

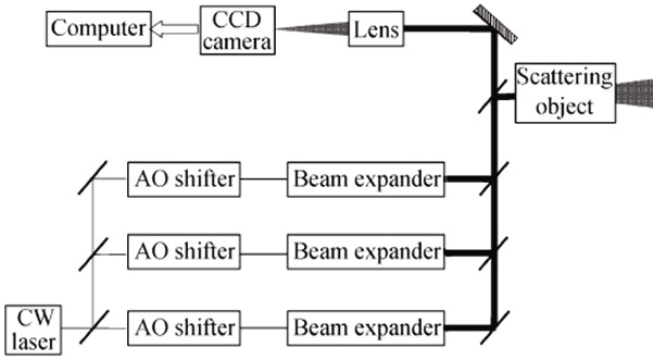

Fig. 4. Optical transmitter.

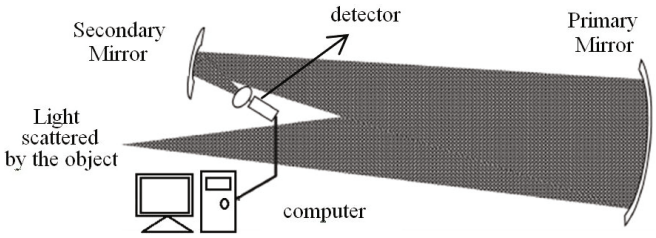

Fig. 5. Optical receiver.

modules of the data acquisition and the spectral estimate are similar to those of the conventional FT. Secondly, the target's information is sparsely represented by means of the wavelet transform and the TV transform, because of which the image can be accurately reconstructed from a small number of observation data far less than those required for the Nyquist-Shannon (N-S) sampling. Thirdly, the target's spectral components are randomly sampled, which can reduce the correlation noise caused by uniform under-sampling. Fourthly, the image is reconstructed by using an optimization model, which ensures that the image can be accurately and quickly reconstructed.

The optimization model of the CS-FT used in this paper is as follows:

$$\min\left\{\|M\cdot F_u\cdot x-y\|^2+\lambda_1\cdot\|W\cdot x\|_1+\lambda_2\cdot TV(x)\right\}. \quad (1)$$

In Eq. (1), x denotes the target image, y denotes the measurement value of the random sparse sampling of the target spectra, M is a randomly sparse sampled template, F_u is the under-sampling Fourier transform operator, W is the wavelet transform operator, λ_1 and λ_2 are regularized parameters. The above optimization model can be considered as a regularized least-squares problem, in which the penalty terms include the sparse prior information of the wavelet transform and the TV transform. In this paper, we use the nonlinear conjugate gradient algorithm [18] to solve the image recovery problem of the CS-FT. For the main procedure of the reconstruction algorithm, the reader may refer to the related paper [18].

IV. COMPARISON OF THE PERFORMANCE OF THE CS-FT AND THE CONVENTIONAL FT

Some brief introductions to both reconstruction methods are shown as follows: The conventional FT method includes reception of the light reflected from target, signal demodulation, phase closure, spectral estimate and image reconstruction. By using the target's spectra obtained with the conventional FT method, the CS-FT method uses the random sampling mode to obtain target's spectra as measurement values, after which the sensing matrix is obtained according to the random sampling mode and the sparse transformation type. Finally, the target's image is reconstructed by using the nonlinear conjugate gradient algorithm.

Here, we give more details about the CS-FT. The nonlinear optimization algorithm of CS-FT is written by Matlab. The wavelet transform operator adopts the Daubechies wavelet function in the Wavelab toolkit. The computer simulation is based on existing codes [24]. During the simulation, the regularized parameters λ_1 and λ_2 are both set to 0.01, and the optimization process uses 8 iterations. The randomly sparse sampled template of the Fourier domain is generated by using the polynomial probability density function and the Monte-Carlo algorithm. This method of using the polynomial probability density function has been proven to be an approximate optimal sampling strategy [18]. Because the target's low-frequency parts have more energy, the low-frequency parts are sampled by using the N-S sampling. A randomly generated template (TSR = 30%, LSR = 10%) is shown in Fig. 3.

Fig. 6. (Color online) Physical layout of transmitter.

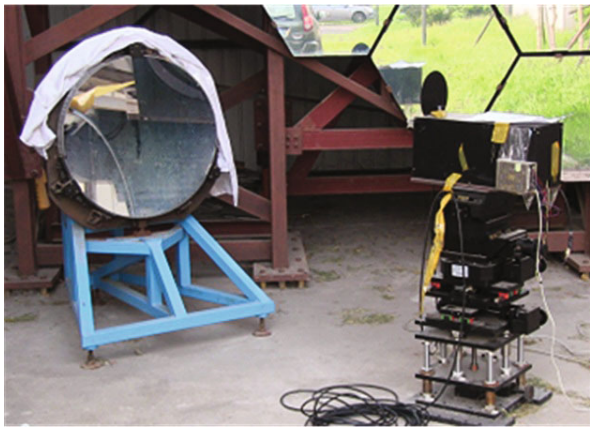

Fig. 7. (Color online) Physical layout of receiver.

1. Field experimental setup

In the actual imaging process, some error sources exist that may not be avoided. These error sources mainly include the beam pointing error, the change of the arrival angle caused by the atmospheric turbulence, the frequency shift of the beam frequency, the laser speckle noise and the particle noise of the detector. Therefore, in the analysis, we use field experimental data which include all of the above error sources to study the influence of the noises on the four methods. Next is a brief introduction to the field experiment devices.

The main purpose of the field experiment is to verify the immunity of the conventional FT to atmospheric turbulence and the influences of actual noise sources on the imaging performance of the FT. The details of the experimental devices can be found in published report [24, 25]. The schemes of the optical transmitter and receiver are shown in Fig. 4 and Fig. 5, respectively. The physical layouts are shown in Fig. 6 and Fig. 7, respectively. In the field experiment, the target is printed on a piece of film as shown in Fig. 8.

Fig. 8. (Color online) Physical picture of the object.

2. Comparison of the imaging quality

In the later analysis and comparison, by changing the LSR and the OPDF, we optimize the image reconstruction process of CS-FT. By changing the TSR, we compare the differences in image quality between the CS-FT and the conventional FT under different compression degrees of the sampled data. The physical meanings and the value ranges of the above three main parameters (LSR, OPDF and TSR) are introduced below.

The parameters LSR and OPDF exist only in variable density sampling. Generally, when sampling with variable density, the spectra of lower frequency are sampled with equal intervals (satisfying the Nyquist sampling theorem), and the spectra of higher frequency are sampled with variable density (that is, the sampling rate with lower frequency is higher, and the sampling rate with higher frequency is lower). The LSR is the ratio of the number of spectra sampled with equal intervals to the number of total sampled spectra (the sum of the spectra sampled with equal intervals and the spectra sampled with variable density). The value range of LSR is [0, 1]. The smaller the LSR is, the smaller the proportion of the sampling with equal intervals is. The OPDF refers to the highest order of the polynomial probability density function selected in variable density sampling. The value ranges of OPDF are positive integers. Generally, positive integers between [3, 10] are chosen. The larger the value is, the faster the sampling rate decreases with increasing spatial frequency. The TSR is the ratio of the number of spectra required by the CS-FT to that required by the conventional FT. The value range of TSR is [0, 1]. A smaller TSR means fewer spectra and shorter imaging time.

In order to quantitatively judge the image quality, we introduce the image's Strehl ratio. The Strehl ratio reflects the similarity between the reconstructed image and the standard image. The closer the Strehl ratio approaches to unity, the closer the reconstructed result approaches to the standard result. The expression for

Fig. 9. Effect of the OPDF: (a) OPDF = 3, (b) OPDF = 4, and (c) OPDF = 5.

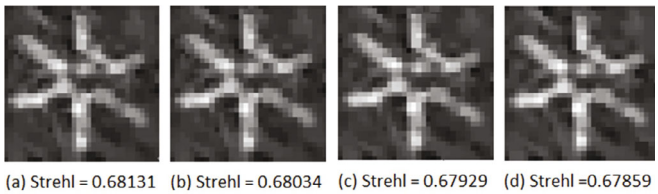

Fig. 10. Effect of the LSR: (a) LSR = 0, (b) LSR = 0.1, (c) LSR = 0.3, and (d) LSR = 0.4.

the Strehl ratio is [24]

$$\text{Strehl} = \frac{\max |O_{\text{std}}(m,n) \otimes O_{\text{cons}}(m,n)|^2}{\iint O^*_{\text{std}}(m,n) O_{\text{std}}(m,n) \mathrm{d}x\mathrm{d}y \iint O^*_{\text{cons}}(m,n) O_{\text{cons}}(m,n) \mathrm{d}m\mathrm{d}n}. \quad (2)$$

In Eq. (2), $O_{\text{std}}(m,n)$ and $O_{\text{cons}}(m,n)$ are the two-dimensional intensity distributions of the standard images and the reconstructed images, respectively, $\otimes$ is the correlation operator, max is the maximum operator and $*$ is the complex conjugate operator.

A. Analysis of the effect of the OPDF

Let TSR = 0.2 and LSR = 0.2. The OPDF is chosen from the numbers 3, 4 and 5, and the reconstruction results are shown in Fig. 9. From Fig. 9, we can see that the reconstruction performance of the CS-FT decreases slightly with increasing OPDF. Therefore, the OPDF should be chosen to be as small as possible.

According to the previous introduction on the OPDF, the smaller the OPDF is, the slower the sampling rate decreases with increasing spatial frequency. The analysis here shows that the object's spectra used in the experiment are mainly concentrated in the low-frequency and medium-frequency bands and the band and that the amount of high-frequency information is less.

B. Analysis of the effect of the LSR

Let TSR = 0.4 and OPDF = 2.6. The LSR is chosen from the numbers 0, 0.1, 0.3 and 0.4, and the reconstruction results are shown in Fig. 10. From Fig. 10, a general trend can be obtained: the reconstruction performance of the CS-FT decreases slightly as the LSR increases. Hence, we should try to choose a smaller LSR.

According to the previous introduction on the LSR, the smaller the LSR is, the smaller the proportion of sampling with equal intervals is. The analysis here shows that the low-frequency information of the object's spectra used in the experiment is not much and that the information is mainly concentrated in the medium-frequency band.

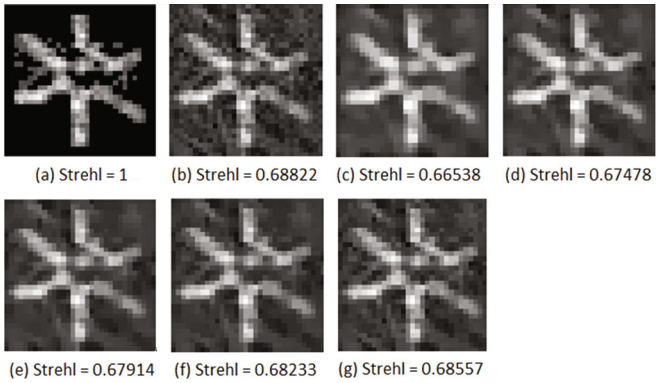

Fig. 11. Effect of the TSR: (a) diffraction limited image, (b) conventional FT result, (c) CS result when TSR = 0.05, (d) CS result when TSR = 0.1, (e) CS result when TSR = 0.2, (f) CS result when TSR = 0.4, and (g) CS result when TSR = 0.8.

C. Analysis of the effect of the TSR

Let LSR = 0 and choose the OPDF to be as small as possible. The TSR is chosen to be a value from 0.05 to 0.8, and the reconstruction results are shown in Fig. 11. From Fig. 11, we can see that the reconstruction performance of the CS increases with increasing TSR. When TSR = 0.8, the reconstruction result of the CS-FT has almost no difference from that of the conventional FT method.

Combining the above three cases, we can get the following conclusions: (I) In the case of the fixed TSR, the smaller the OPDF is, the better the reconstruction performance of CS-FT is. (II) When the LSR is smaller, the reconstruction results of the CS-FT are better. (III) As the TSR increases, the reconstruction results of the CS-FT are improved. When TSR = 0.8, the differences in the results for the two methods are very small.

3. Analysis of the imaging time

The Fourier telescope is known as an imaging system with a post-processing procedure, which first utilizes the optical receiver to obtain all the echoes from the target

and then reconstructs the image by using a reconstruction algorithm. The imaging time of the Fourier telescope includes the time of target information acquisition (TIA) and the time of image reconstruction.

The process of TIA is mainly divided into several steps, such as the telescope movement, tracking and aiming, the beam switching and phase compensation, and so on. The conventional FT acquires the target information from multiple laser transmissions (each time to acquire a new frequency component of the target). The time of each operation is about 15 seconds, so the whole process of TIA takes a long time. Next, we take the conventional FT, which simultaneously transmits three laser beams each time, as an example to calculate the time of TIA. In order to obtain $33 * 33$ resolution of the target image, the conventional FT needs to measure the $33 * 33$ spectral components of the target. As the Fourier transform of the real function has a characteristic of conjugation, it only needs to measure half of the above spectra (about 545 components). Therefore, the time needed to get information from the target is about $545 * 15 = 8175$ (seconds) ≈ 2.27 (hours).

The process of image reconstruction mainly includes several steps, such as the information demodulation, the phase closure, the spectrum estimate and the image recovery. For a target with $33 * 33$ resolution, the reconstruction time of the conventional FT is about 114 seconds, much less than the time of TIA (about 8175 seconds). Therefore, the decrease of the time of TIA is the key to reduce the overall imaging time of the Fourier telescope.

The CS-FT can effectively reduce the time of TIA, but slightly increasing the reconstruction time by only a little more than 20 seconds, which means that this method can effectively reduce the total imaging time of the Fourier telescope. The imaging times of the conventional FT and the CS-FT are compared for different TSRs in Table 1. Table 1 shows that for a decreasing total sampling rate, the imaging time of the CS-FT is decreased significantly. If the TSR can be chosen reasonably, the CS-FT can not only significantly reduce the imaging time, but also ensure that its imaging quality is close to that of the conventional FT.

Table 1. Comparison of the conventional FT and the CS-FT.

TSR	Conventional FT (s)	CS method (s)
0.05	8289	554
0.1	8289	968
0.2	8289	1797
0.4	8289	3455
0.8	8289	6771

V. CONCLUSION

From the above analyses, we can draw the following conclusions:

(I) For the CS-FT, the smaller values of the LSR ($\mathrm{LSR} = 0$) and the OPDF ($\mathrm{OPDF} = 3$) can be used to achieve a better image quality. This also shows that the object's information used in this paper is mainly concentrated in the mid-frequency band.

(II) With decreasing the total sampling rate, the imaging time of the CS-FT decreases significantly. If the TSR can be chosen reasonably, the CS-FT can not only significantly reduce the imaging time, but also ensure that its imaging quality is close to that of the conventional FT.

(III) The data from the above analyses are derived from a field experiment, which means that the above reconstruction methods can be used in an actual noisy situation that the conclusions of this paper can be used effectively to guide actual imaging applications.

Of course, the current research of the CS-FT is still in the early stage, so many aspects, such as how to choose a reasonable configuration of transmitting baselines to adapt to the random under-sampling of the target spectra, whether the discontinuance of transmitting baselines significantly decreases the imaging performance, *etc*, need to be studied. Therefore, we will continue to work to overcome the above obstacles to the final realization of the actual imaging application of CS-FT.

ACKNOWLEDGMENTS

The authors acknowledge the financial support from the National Natural Science Foundation of China [Grant No. 11703024] and the Excellent Young Scientists Fund of the Science and Technology Development Foundation of Jilin Province, China [Grant No. 20180520 076JH].

REFERENCES

[1] L. Sica, Appl. Opt. **30**, 206 (1991).
[2] B. F. Campbell, L. Rubin and R. B. Holmes, Appl. Opt. **34**, 5932 (1995).
[3] C. D. Rider, C. Jingle and E. Nielson, in *Proceeding of the 1996 Space Surveillance Work Group* (MIT Lincoln Laboratory, Massachusetts, 1996), p. 147.
[4] R. B. Holmes *et al.*, J. Opt. Soc. Am. A **13**, 351 (1996).
[5] T. J. Brinkley and D. Sandler, Proc. SPIE **3815**, 42 (1999).
[6] A. B. Peter and I. M. Valery, Proc. SPIE **3815**, 49 (1999).
[7] E. L. Cuellar, J. Stapp and J. Cooper, Proc. SPIE **5896**, D1 (2005).
[8] I. M. Valery, A. B. Peter and I. G. Victor, Proc. SPIE **4167**, 192 (2001).

[9] B. Mikhail *et al.*, Proc. SPIE **4821**, 62 (2002).
[10] D. F. Stephen *et al.*, Proc. SPIE **3815**, 2 (1999).
[11] V. L. Gamiz *et al.*, Proc. SPIE **4091**, 304 (2000).
[12] A. T. Marcia *et al.*, Proc. SPIE **4489**, 78 (2002).
[13] J. Stapp *et al.*, Proc. SPIE **6307**, 01-1 (2006).
[14] B. Spivey, J. Stapp and D. Sandler, Proc. SPIE **6307**, 02-1 (2006).
[15] E. L. Cuellar *et al.*, Proc. SPIE **7094**, 0G-1 (2008).
[16] E. J. Candes and M. B. Wakin, IEEE Signal Process. Mag. **25**, 21 (2008).
[17] J. Romberg, IEEE Signal Process. Mag. **25**, 14 (2008).
[18] M. Lustig, D. Donoho and J. M. Pauly, Magn. Reson. Med. **58**, 1182 (2007).
[19] D. Qi and W. E. I. Sha, Mathematics **1**, 1 (2009).
[20] X. Qu *et al.*, Inverse Probl. Sci. Engin. **18**, 737 (2010).
[21] C. Lu *et al.*, Proc. SPIE **8551**, 10-1 (2012).
[22] Y. Li *et al.*, Proc. SPIE **8877**, 0J-1 (2013).
[23] Z. Zhou *et al.*, Optik **124**, 5542 (2013).
[24] S. Yu *et al.*, Appl. Opt. **55**, 6654 (2016).
[25] L. Dong *et al.*, Acta Opt. Sin. **32**, 0201004-1 (2012).